

# Forest understory plant and soil microbial response to an experimentally induced drought and heat-pulse event: the importance of maintaining the continuum

ISABELL VON REIN<sup>1</sup>, ARTHUR GESSLER<sup>1,2,3</sup>, KATRIN PREMKE<sup>1,4</sup>, CLAUDIA KEITEL<sup>5</sup>, ANDREAS ULRICH<sup>1</sup> and ZACHARY E. KAYLER<sup>1</sup>

<sup>1</sup>Institute for Landscape Biogeochemistry, Leibniz Centre for Agricultural Landscape Research (ZALF), 15374 Müncheberg, Germany, <sup>2</sup>Berlin-Brandenburg Institute of Advanced Biodiversity Research (BBIB), Altensteinstr 6, D-14195 Berlin, Germany, <sup>3</sup>Swiss Federal Institute for Forest, Snow and Landscape Research (WSL), Zürcherstr 111, CH-8903, Birmensdorf, Switzerland, <sup>4</sup>Leibniz-Institute of Freshwater Ecology and Inland Fisheries, Chemical Analytics and Biogeochemistry Müggelseedamm 310, 12587 Berlin, Germany <sup>5</sup>Centre for Carbon, Water and Food, Faculty of Agriculture & Environment, university of sydney, 380 Werombi Rd, Brownlow Hill, NSW 2570, Australia

## Abstract

Drought duration and intensity are expected to increase with global climate change. How changes in water availability and temperature affect the combined plant–soil–microorganism response remains uncertain. We excavated soil monoliths from a beech (*Fagus sylvatica* L.) forest, thus keeping the understory plant–microbe communities intact, imposed an extreme climate event, consisting of drought and/or a single heat-pulse event, and followed microbial community dynamics over a time period of 28 days. During the treatment, we labeled the canopy with <sup>13</sup>CO<sub>2</sub> with the goal of (i) determining the strength of plant–microbe carbon linkages under control, drought, heat and heat–drought treatments and (ii) characterizing microbial groups that are tightly linked to the plant–soil carbon continuum based on <sup>13</sup>C-labeled PLFAs. Additionally, we used 16S rRNA sequencing of bacteria from the Ah horizon to determine the short-term changes in the active microbial community. The treatments did not sever within-plant transport over the experiment, and carbon sinks belowground were still active. Based on the relative distribution of labeled carbon to roots and microbial PLFAs, we determined that soil microbes appear to have a stronger carbon sink strength during environmental stress. High-throughput sequencing of the 16S rRNA revealed multiple trajectories in microbial community shifts within the different treatments. Heat in combination with drought had a clear negative effect on microbial diversity and resulted in a distinct shift in the microbial community structure that also corresponded to the lowest level of label found in the PLFAs. Hence, the strongest changes in microbial abundances occurred in the heat–drought treatment where plants were most severely affected. Our study suggests that many of the shifts in the microbial communities that we might expect from extreme environmental stress will result from the plant–soil–microbial dynamics rather than from direct effects of drought and heat on soil microbes alone.

**Keywords:** <sup>13</sup>CO<sub>2</sub> pulse labeling, 16S rRNA next-generation sequencing, climate extremes, drought, forest understory, heat-pulse, microbial community structure, plant–soil–microbe carbon continuum, PLFAs

Received 15 January 2016; revised version received 15 January 2016 and accepted 22 February 2016

## Introduction

Current and impending climate change is predicted to result in modified temperature and precipitation regimes causing potentially severe alterations of ecosystem functioning, biogeochemistry and community patterns (IPCC, 2012; Reichstein *et al.*, 2013; Bahn *et al.*,

2014). In Europe, the frequency, duration, and intensity of droughts and heat waves are expected to increase (Schar *et al.*, 2004; Beniston *et al.*, 2007; Briffa *et al.*, 2009; Fischer & Schar, 2010) and evidence of climate change impacts on important ecosystem properties, functions and services is emerging. These include shifts in phenology (Menzel *et al.*, 2006), animal and plant species' distribution (Walther *et al.*, 2002) and primary productivity (Ciais *et al.*, 2005). But other responses, such as microbial community shifts, are not readily apparent, ostensibly due to a high level of microbial phenotypic plasticity (Merilä & Hendry, 2014), functional redundancy within soil communities (Lennon *et al.*, 2012; Griffiths & Philippot, 2013) and distinctive

Correspondence: Present address: Zachary Kayler, Northern Research Station, Lawrence Livermore National Laboratory, USDA Forest Service, Livermore, CA 94550, USA, tel. +1 925 423 4537, fax +1 925 423 7884, e-mail: zkayler@fs.fed.us; Andreas Ulrich, tel. +49 033432 82 345, fax: +49 033432 82 343, e-mail: ulrich@zalf.de

resistance and resilience of soil microorganisms (Shade *et al.*, 2012; Griffiths & Philippot, 2013).

Species, communities and ecosystems have revealed a strong tolerance or resistance to a wide range of environmental variation (Scheffer & Carpenter, 2003; Lennon *et al.*, 2012; Placella *et al.*, 2012; Manzoni *et al.*, 2014). Accordingly, not all experiments designed to simulate climate change have resulted in a corresponding response from the community or ecosystem (Smith, 2011; Hoover *et al.*, 2014), which is why ecological researchers have recently focused on experiments that induce extreme climate events with the goal of identifying critical thresholds and their underlying mechanisms (Reichstein *et al.*, 2013; Kayler *et al.*, 2015). Smith (2011) defined a climate extreme as a statistically rare event that can 'alter ecosystem structure and/or function well outside the bounds of what is considered typical or normal variability'. Research based on extreme events has already yielded insights into belowground dynamics (Evans & Wallenstein, 2014), but these experiments have largely been carried out using laboratory soil incubations (Barcenas-Moreno *et al.*, 2009; Riah-Anglet *et al.*, 2015), thus separating linkages between vegetation and soil microbes. Important questions remain about the relevance of the plant–soil–microorganism carbon continuum in extreme climate event scenarios, including at which point (i.e., threshold) is the plant–soil–microorganism connectivity lost? And, how will microbial communities respond when pushed to their niche limits?

Plants influence microbial communities and functions in multiple ways. Plant effects include the amelioration of the environment, such as soil temperature and moisture (Waldrop & Firestone, 2006), physiological and life strategies of plants that influence litter quality (Hobbie, 1992; Aerts, 1997; Prescott & Grayston, 2013), and carbon allocation patterns (Litton *et al.*, 2007). Soil microbial community function, on the other hand, can regulate plant diversity–productivity patterns (Van Der Heijden *et al.*, 2008; Schnitzer *et al.*, 2010; Schnitzer & Klironomos, 2011), nutrient availability and cycling (Bonkowski & Roy, 2005; Wagg *et al.*, 2014), and may even boost plant fitness to environmental stress or affect their evolution (Lau & Lennon, 2011). Whether top-down or bottom-up control is at play, important ecosystem functions result from the plant–soil–microorganism continuum (Bardgett *et al.*, 2005; Gilliam *et al.*, 2014), which is often severed due to changes in temperature and precipitation regimes (Evans & Wallenstein, 2014).

Drought and heat stress can impact soil microorganisms through both direct (e.g., modification of soil structure and pore connectivity in soils) and indirect effects (e.g., reduction in plant net primary productivity resulting in lower microbial C availability) (Bardgett *et al.*, 2008). Drought has a strong influence on carbon

assimilation in plants, affecting stomatal and mesophyll conductance (Hommel *et al.*, 2014), leaf biochemistry and hydraulic pathways (Flexas *et al.*, 2006; Resco *et al.*, 2009), as well as phloem loading which can result in a reduction in the carbon transfer from the plant canopy to the roots and to soil microorganisms (Ruehr *et al.*, 2009). Additional to the reduction in carbon input from plants into the soil (an indirect effect of climate change), mass transfer of reduced substrates within the soil (e.g., dissolved organic carbon) to microbial communities slows (a direct effect of climate change) due to diminished pore connectivity in dry soil (Schimel & Schaeffer, 2012; Manzoni *et al.*, 2014). The reduction in soil moisture also limits the ability of microbes to migrate to available substrates (Manzoni *et al.*, 2014) or can alter the chemistry of the soil (e.g., acidification) affecting carbon turnover (Clark *et al.*, 2005). A soil water potential of  $-14$  MPa, far below the permanent wilting point for plants, has been suggested as the level at which substrate availability to microorganisms is limited by mass transfer (Manzoni *et al.*, 2011). With linkages to plants severed resulting in a reduced supply of plant-derived assimilates, microbes can alter their physiology (Csonka, 1989; Allison *et al.*, 2010; Crowther *et al.*, 2014) and/or change their carbon allocation (Schimel & Schaeffer, 2012), for example, by producing extracellular enzymes or accumulating osmolytes to maintain cell integrity (Csonka, 1989; Schimel *et al.*, 2007).

Observations and syntheses of microbial community response to climate change, including drying and warming, are emerging; however, resolving stress-response strategies of microorganisms remains an ongoing challenge in environmental microbiology (Schimel *et al.*, 2007; Lennon *et al.*, 2012; Evans & Wallenstein, 2014). For example, fungi have been shown to have a high tolerance for water stress, often attributed to their ability to spatially explore the soil better for water and nutrients (Frey *et al.*, 2008; Riah-Anglet *et al.*, 2015). Additionally, due to their differences in cell wall structure, fungi and gram-positive bacteria (which have a thick, interlinked peptidoglycan cell wall) are considered to have wide niche breadths with respect to soil moisture ranges and a stronger tolerance to desiccation (Schimel *et al.*, 2007; Lennon *et al.*, 2012). Yet, given the multiple and often conflicting community changes observed with modern sequencing tools, generalizations remain elusive, although it is interesting that ecological strategies appear to be grouped at a coarse taxonomic level (phylum) (Lennon *et al.*, 2012).

To understand how the plant–soil–microorganism continuum responds to impending climate change, including climate extremes, we need to maintain the plant–soil carbon continuum and push the plant and microbial communities beyond their current evolution-

ary niche boundaries (Bahn *et al.*, 2014; Kayler *et al.*, 2015). We excavated monoliths from a beech (*F. sylvatica* L.) forest in Germany, thus keeping the understory plant–microorganism communities intact, and imposed an extreme climate event, consisting of drought and/or a single heat-pulse event. During the treatment, we labeled the understory vegetation with  $^{13}\text{CO}_2$  and then followed microbial community dynamics over a short time period of 28 days. Our overarching goal was to understand how the forest understory may react to future climate change, by balancing the simplicity of a short-term extreme climate event in a semi-controlled environment with the complexity of the plant–soil–microorganism system response, focusing on plant–microorganism linkages and changes in microbial community structure. Specific aims and hypotheses of the study were as follows:

- 1 Characterize the carbon transport dynamics by studying the relative arrival events of labeled assimilates to belowground plant tissues and microbial phospholipid-derived fatty acids (PLFA), allowing the assessment of the strength of plant–microbe linkages under the different treatments. Based on the label patterns, we hypothesize (i) that the extreme temperature and heat treatments will result in the plant–soil microbial community linkage to be severed.
- 2 Characterize metabolically active soil microorganisms using  $^{13}\text{C}$ -labeled isotopic PLFAs that are tightly linked to the plant–soil carbon continuum as the environmental stress increases. Implicit to the canopy labeling is the hypothesis (ii) that the drought and heat-stressed treatments will lead to a lower  $^{13}\text{C}$  label in the PLFAs relative to those from the well-watered control and will be near absent when the carbon continuum is completely severed.
- 3 Determine the short-term changes in the community structure of the metabolically active bacteria to the stress treatments and the related changes in plant assimilate transfer belowground, using high-throughput sequencing of the 16S rRNA of bacteria from the Ah horizon of the soil. We hypothesize (iii) that if the treatments result in primarily indirect climate effects then we will observe a shift in the bacterial community that directly corresponds to the treatment effect on the understory vegetation.

## Materials and Methods

### Experimental strategy

We excavated 20 intact soil monoliths ( $50 \times 50 \times 20$  cm,  $L \times W \times D$ ) from a beech forest understory and transported

them to a greenhouse. After acclimatization to the greenhouse conditions, the monoliths were separated into soil moisture treatments (well-watered control and drought). To ease the logistics of the experiment, we performed two isotopic labeling events separated by 14 days. During the second labeling event, outside ambient temperatures increased, resulting in a rise in the average chamber temperature and a maximum chamber temperature of  $50^\circ\text{C}$  was recorded. We view this as a serendipitous event that provided us with an opportunity to test the effects of drought and drought plus strongly increased temperature (a heat-pulse) on the plant and soil microbial communities. Thus, our treatments ( $n = 5$ ) are well-watered control (C), drought (D), well-watered heat-pulse (H) and heat-pulse with drought (HD).

C and H treatment monoliths were watered constantly to field capacity, whereas the D and HD monoliths did not receive any water after the treatment onset. Due to the separation of the experiment into two stages, the acclimatization time of the soil monoliths to greenhouse conditions was 11 days before drought was initiated for the first labeling consisting of the C and D treatment, while the soil monoliths of the H and HD treatment had 25 days to acclimatize before the start of the drought treatment. The experimental treatments lasted a total of 28 days for all monoliths, and the  $^{13}\text{CO}_2$  labeling was performed on day 13 after the onset of the drought treatment.

### Monolith sampling and setup

The twenty soil monoliths were excavated with their natural understory vegetation in June from a managed beech (*F. sylvatica* L.) stand in the Hainich forest near Kammerforst, Germany ( $51^\circ06'\text{N}$ ,  $10^\circ23'\text{E}$ ). The annual mean temperature and precipitation in our sample area are  $6.5\text{--}7.5^\circ\text{C}$  and 750–800 mm, respectively. The soil types of the Hainich Forest are Luvisols and Stagnosols (Fischer *et al.*, 2010) and the monoliths were sampled within a 100 m radius, thus assuring similar general soil properties (e.g., soil parent material, forest management influences). The monolith understory contained woodruff (*Galium odoratum*), young common ash (*Fraxinus excelsior*) and wood sorrel (*Oxalis acetosella*), among others (Table S1).

In the field, the monoliths were placed in wooden boxes that were constructed with a drainage hole in the bottom. In the greenhouse, monoliths were placed underneath a shade cloth and quartz sand was used to fill in gaps along the edges between the soil and wooden box. We measured the greenhouse air temperature continuously ( $T_{\text{Air}}$ ; Kombisensor KS 550; ELV Elektronik AG, Leer, Germany), soil moisture content on all monoliths (ECH2O EC-5; Decagon Devices Inc., Pullman, WA, USA) and soil temperature ( $T_{\text{Soil}}$ ; Model 109 Temperature Probe; Campbell Scientific Inc., Logan, UT, USA) on a subset of monoliths ( $n = 3$ ). The soil moisture is given in mean-% values compared to the maximum water-holding capacity (%max) for each treatment ( $n = 5$ ). A light sensor (QSO-S PAR Photon Flux sensor; Decagon Devices Inc.) and a relative humidity sensor (VP-3 sensor; Decagon Devices Inc.) were installed under the shade cloth. We calculated soil pore

water potential (kPa) by calibrating the soil moisture probe measure content against a pF curve (19.6 kPa). For values of pore water potential beyond the pF curve, we fit (Seki, 2007) the pressure and soil moisture values to the model of Van Genuchten (1980). Soil  $^{13}\text{C}$  measurements were conducted by placing a  $\text{CO}_2$  permeable membrane (8 cm, ACCUREL PP V8/2HF; Membrana GmbH, Wuppertal, Germany) vertically inside each monolith at 10 cm depth. The membrane was connected to a polyethylene tube placed vertically through the monolith. Soil gas pumped through the tubing ( $1 \text{ l min}^{-1}$ ) was monitored with a  $^{13}\text{C}$  cavity ring down spectrometer (Picarro G2101-i, Santa Clara, CA, USA).

### Sample collection

Soil, aboveground plant tissues (pooled samples from leaves and stems) and coarse roots were sampled at 0, 6, 12, 14, 21 and 28 days after the drought began [Drought Day (DD) 0, 6, 12, 14, 21 and 28]. Soil samples were extracted from the Ah horizon using a cork borer ( $\text{Ø} 5 \text{ mm}$ ). For  $\delta^{13}\text{C}$  analysis of plant organic matter, we used plant material from all six sampling events; for  $^{13}\text{C}$ -PLFA analysis, we used soil from five sampling events (without DD 6); and for 16S rRNA-based sequencing, we used soil from 3 samplings (DD 0, 14, 28). We sampled the plant species *Galium odoratum* for isotopic analysis because it was the most common plant growing on the monoliths. *Oxalis acetosella* was sampled when *Galium odoratum* was absent. For all soil and plant samples, five randomly distributed subsamples from spatially different points within the monoliths were compiled. The samples were stored at  $-80^\circ\text{C}$  until analysis.

### Labeling

We performed two labeling events with 10 monoliths per event. After 2 weeks of drought, the vegetation of the monoliths was pulse-labeled with  $^{13}\text{C}$  on July 8 (1st event; labeling of C and D) and July 22 (2nd event; labeling of H and HD). A gastight chamber was placed over the monoliths to avoid leakage of  $^{13}\text{C}$  into the atmosphere. The  $^{13}\text{C}$  was produced by adding 80%  $\text{H}_3\text{PO}_4$  (in excess) to 99%  $^{13}\text{C}$ -enriched sodium bicarbonate (>99.9%  $\text{CO}_2$  with 99 atom-%  $^{13}\text{C}$ ; Cambridge Isotope Laboratories, Andover, MA, USA). In the second labeling event vegetation within the HD treatment wilted (pictures see Fig. S1), consequently we increased the amount of label to ensure PLFA labeling (13 g vs. 5 g used in the C and D treatment). Fans inside the roof dispersed the generated gas. The roof was removed after eight hours of  $^{13}\text{C}$  fumigation.

### Isotopic analysis

Aboveground plant tissues, roots and soil were dried for 48 h at  $60^\circ\text{C}$ , then ground to a homogenous powder. The isotopic composition of the bulk plant and soil samples was analyzed at the ZALF Isotope Core Facilities by combusting 0.3–0.5 mg of the ground material in an elemental analyzer (Flash HT Elemental Analyzer; Thermo Fisher Scientific,

Waltham, MA, USA) coupled to an Isotopic Ratio Mass Spectrometer (Delta V Advantage IRMS; Thermo-Scientific). The isotopic values are expressed in delta notation (in ‰ units), relative to VPDB (Vienna Pee Dee Belemnite) and calibration was to IAEA-CH-6 (sucrose) and USGS40 (L-glutamic acid). Analysis of internal laboratory standards ensured that the estimates of the organic isotopic values were precise to within  $0.1\text{‰}$ .

For phospholipid fatty acid (PLFA) extraction, soil samples were freeze-dried and 1 g of dry soil was extracted with a modified one-phase Bligh/Dyer method (Frostegård *et al.*, 1991; Steger *et al.*, 2011). The lipids were then separated into different lipid classes with increasing polarity (neutral, glyco- and phospholipids) using solid phase extraction with silicic acid columns (BondElut LRC-Si; Agilent Technologies Inc., Santa Clara, CA, USA). The fatty acid heneicosanoic acid (21 : 0) was added to the samples as an internal standard. The PLFA samples were dried and stored at  $-20^\circ\text{C}$  until analysis. Quantification and identification of PLFAs was performed on a GC (Steger *et al.*, 2011). We used standard nomenclature to refer to the PLFAs (Boschker *et al.*, 2005; Kaur *et al.*, 2005; Denef *et al.*, 2009; Steger *et al.*, 2011).

The stable carbon-isotopic composition of the individual PLFAs was determined on a Thermo-Scientific GC/C-IRMS system (Thermo Trace GC Ultra gas chromatograph coupled to a Delta V Advantage IRMS) at the UC Davis Stable Isotope Facility. PLFA  $\delta^{13}\text{C}$  data were corrected for the addition of the methyl group by mass balance and were calibrated by our own internal and external fatty acid methyl ester (FAME) standards. Stable carbon isotope ratios are reported on the VPDB scale.

The  $^{13}\text{C}$  uptake into the microbial PLFA biomass is expressed as excess  $^{13}\text{C}_{\text{PLFA}}$  [ $\mu\text{g C} \times \text{kg}^{-1}$ ]. The excess  $^{13}\text{C}_{\text{PLFA}}$  represents the total amount of  $^{13}\text{C}$  in the microbial PLFAs per kilogram soil and is calculated as follows (Fuchslueger *et al.*, 2014):

$$\frac{(\text{atom}\%_{\text{Sample}} - \text{atom}\%_{\text{NA}} * \text{Biomass}[\mu\text{g C}])}{100} * 1000 [\text{g}] \quad (1)$$

in which  $\text{atom}\%_{\text{Sample}}$  is the atom% of the labeled PLFA sample,  $\text{atom}\%_{\text{NA}}$  is the atom% of the PLFA sample 1 day before labeling (representing natural abundance of  $^{13}\text{C}$ ), and Biomass is the PLFA biomass [ $\mu\text{g C}$ ].

### RNA extraction and amplicon high-throughput sequencing

Total DNA and RNA were co-extracted from 100 mg soil (Ah horizon) (for extraction methods see Felsmann *et al.*, 2015). We used MiSeq-based (Illumina Inc., San Diego, CA, USA) high-throughput sequencing to analyze the metabolically active (RNA-based) soil bacterial communities. We amplified cDNA samples with primers 8f and Eub518 targeting the V1–V3 region of the bacterial 16S rRNA gene. At their 5' end, the reverse primers carried a specific 6–7 nt barcode and a 2 nt linker for each soil sample. The barcodes differed in at least 2 nt and were selected from those applied by Schloss *et al.* (2011). Two independent PCR reactions were performed using

AccuPrime Taq High Fidelity (Invitrogen, Carlsbad, CA, USA). Cycling conditions were an initial denaturation of 1 min at 94 °C, followed by 23 cycles of 20 s at 94 °C, 30 s at 53 °C and 90 s at 72 °C, and a final extension of 7 min at 72 °C. Combined amplicons were purified with the MSB Spin PCRapace kit (Invitex, Berlin, Germany), quantified using a Qubit fluorometer (Life Technologies, Darmstadt, Germany) and pooled to achieve a mixed sample with equimolar amounts of all PCR products. Adapter ligation and amplicon sequencing of 300-bp paired ends were carried out by GATC (Konstanz, Germany).

We used the software package Mothur v. 1.30.2 (Schloss *et al.*, 2009) to process raw sequences. Paired sequences were used to make contigs and optimized by trimming off primer and barcode sequences (primer differences allowed, 2 bp, barcodes, 1 bp) and by removing sequences with mismatched nucleotides that differed by less than six units between the quality scores of both reads. To remove potential sequencing noise, reads differing by less than 1% of total residues were grouped by single linkage preclustering (Huse *et al.*, 2010) and singletons were discarded as suggested in the UPARSE pipeline (Edgar, 2013). High-quality reads were aligned using the SILVA database, and chimeras were removed using the Uchime algorithm (Edgar *et al.*, 2011). After calculation of a distance matrix, operational taxonomic units (OTU) were generated using a cutoff of 0.03. For phylogenetic identification, the sequences were compared to the RDP 16S rRNA training set 10 using a confidence threshold of 80%. To equalize the number of sequences per sample, each group of sequences was subsampled to the size of the smallest group. Sequences were deposited in the NCBI Short Read Archive (SRP059718 and SRP059783).

### Statistical analysis

Treatment differences in environmental (water-holding capacity, soil water potential, soil temperature) and isotopic values (leaves, stems, roots) were tested using a repeated measures ANOVA followed by a Tukey's HSD test. Statistical analysis was carried out in R version 2.15.1 (R Development Core Team, 2008). For the sequencing results, we used nonmetric multidimensional scaling (NMS) analysis to detect shifts in the bacterial community structure in which the relative proportion of OTUs within each sample was used as input for calculating NMS by PC-ORD v.6.08 (McCune & Mefford, 2011). We implemented the Bray–Curtis distance measure to construct the NMS, which does not overemphasize the variance of low-abundant OTUs. Stress values were in the range of 8.2% and 9.2%, indicating a reliable test performance (Clarke, 1993). We used a multi-response permutation procedure (MRPP) (Mielke & Berry, 2007) to identify significant differences in the bacterial communities over time and between treatments. MRPP reports a chance-corrected within-group agreement ( $A$ ) that describes the observed within-group homogeneity to the random expectation (i.e.,  $A = 1$  when communities within a treatment are identical and  $A < 0$  when there is less agreement within the treatments than expected by chance (McCune and Grace, 2002).

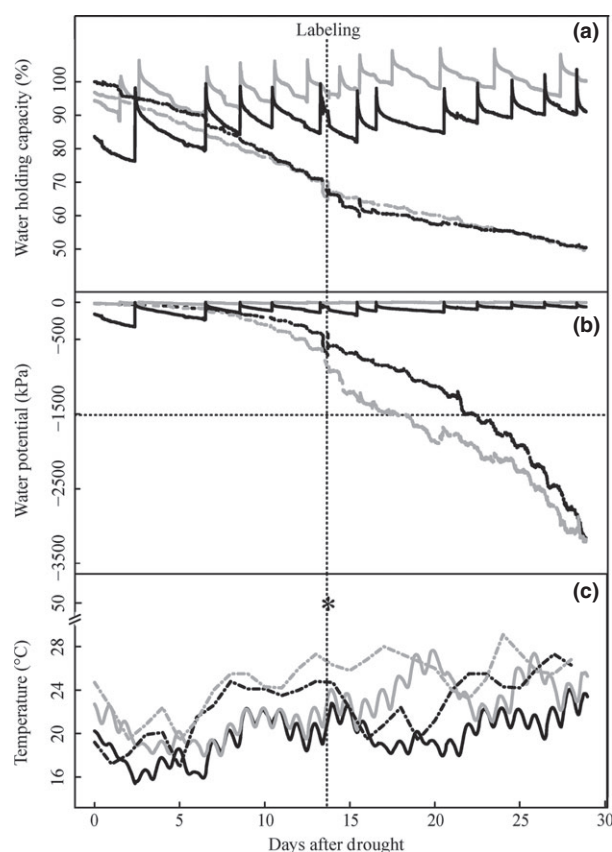


**Fig. 1** Water-holding capacity (%), soil pore water potential (kPa) and temperature (°C) during the experiment: (a) percent of the mean maximum water-holding capacity in well-watered control (C; black solid line) and heat (H; gray solid line) and nonwatered drought (D; black dotted line) and heat–drought (HD; gray dotted line); (b) soil pore water potential (kPa) during the experiment (legend as above) with horizontal dotted line indicating permanent wilting point and (c) air temperature in dotted lines [ $T_{\text{air}}$ ; daily mean value of 15 min interval measurements (°C)] and soil temperature in solid lines [hourly  $T_{\text{soil}}$  (°C)] for C and D (black) and H and HD (gray);  $n = 5$  for each treatment. \*Indicates the maximum temperature inside the roof during the second labeling.

## Results

### Greenhouse conditions and soil water potential

Figure 1a and b shows the soil moisture (SM) as water-holding capacity (%) and water potential ( $\psi$ ) in kPa over the experiment. At the beginning of the experiment, all treatments were at or near 100% $_{\text{max}}$  (SM) and soil water potential was near 0 kPa, indicating that all treatments were well-watered. The C and H treatment remained at these levels throughout the duration of the experiment. In the D and HD treatments, the soil moisture and water potential gradually

decreased from the beginning of the experiment and SM reached 65%<sub>max</sub> at the time of labeling (after 2 weeks of drought). Permanent wilting point in D was reached after DD 22 and in the HD treatment after DD 18. By the end of the 28-day experiment, SM was reduced below 48%<sub>max</sub> and  $\psi$  below  $-3250$  kPa in both treatments.

Mean daily air temperatures ( $T_{\text{air}}$ ) in total varied between 17 and 31 °C during the experiment and mean daily soil temperatures ( $T_{\text{soil}}$ ) between 16 and 27 °C (Fig. 1c). During the H and HD treatment, an increased air and soil temperature was observed over time. Nine days (from 28) were significantly warmer by at least 4.6 °C ( $P < 0.001$ ) when compared to the C and D treatment and 23 days had significantly warmer soil temperatures by 1 to up to 7 °C ( $P < 0.05$  and  $< 0.001$ ). During the second labeling, the temperature inside the chamber substantially increased (up to 50 °C) as the labeling was performed outside the greenhouse with ambient temperatures approaching 40 °C by midday. Therefore, we increased the available concentration of  $^{13}\text{CO}_2$  to compensate for the reduction in the functional leaf area (Fig. S1) that occurred during the heat-pulse; however, given the relative similar values in label of the D and HD plant samples, we infer that plant uptake, and not the amount of  $^{13}\text{CO}_2$ , is what ultimately controlled the amount of label in the plant–soil continuum.

#### Plant and soil isotopic patterns

Before labeling, mean  $\delta^{13}\text{C}$ -values ranged from  $-32.6\text{‰}$  to  $-31.1\text{‰}$  in leaf and stem tissues and from  $-32.5\text{‰}$  to  $-30.3\text{‰}$  in roots. Compared to the natural abundance levels before labeling, all treatments were significantly enriched in  $^{13}\text{C}$  ( $P < 0.05$ ) (Fig. 2a). Comparisons across the treatments show that C and H followed the same label dynamics, while there was a significant difference between C and D initially (DD 14), and a significant difference between HD and D on DD 21 ( $P < 0.05$ ). The  $\delta^{13}\text{C}$  in aboveground tissue tended to decrease between the day after labeling (DD 14) and 7 days later (DD 21); values decreased by 61.2% (C), 62.2% (D), 40.4% (H) and 8% (HD), but only the decrease in the control was significant ( $P < 0.01$ ). The  $^{13}\text{CO}_2$  canopy fumigation successfully labeled root biomass within all treatments (pre vs. post label,  $P < 0.01$ ). However, the increase was not significant between the treatments (Fig. 2b), most likely due to the high spatial variability of the label within the monoliths. The maximum  $\delta^{13}\text{C}$ -value ( $146.33\text{‰} \pm \text{SE } 25\text{‰}$ ) for the roots was found in the control 15 days after labeling (DD 28).

We monitored  $^{13}\text{CO}_2$  isotopic composition in the labeling chamber during the labeling and in the soil gas for 5 days after labeling. The purpose of these values

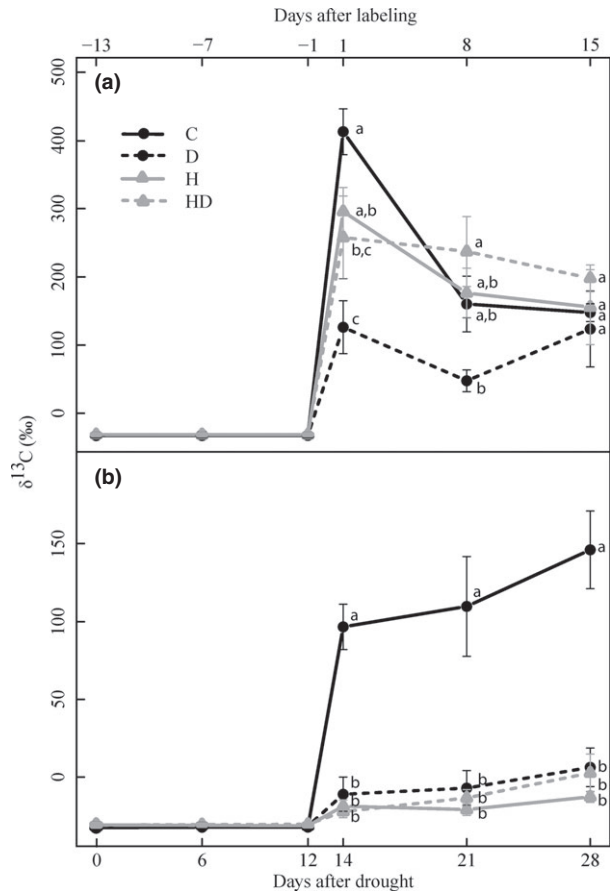


**Fig. 2** Fate of the  $^{13}\text{C}$  label for (a) aboveground tissues (leaves and stems) and (b) roots of *Galium odoratum* in the control (C), drought (D), heat-pulse (H) and heat-pulse with drought (HD) treatments as  $\delta^{13}\text{C}$  values (‰) during the experiment – with the upper x-axis showing days before (negative values) and days after labeling (positive values) and the lower x-axis showing days after the onset of the drought treatment. Values are means  $\pm$  SE ( $n = 5$ ). Significances are indicated separately for each time point.

was primarily to assess the arrival of label rather than to quantify fluxes. In general, we could detect a pulse of labeled carbon present in soil  $^{13}\text{CO}_2$  after 1 day in C and after 2 days in HD (Fig. S2). We could not determine the soil  $^{13}\text{CO}_2$  dynamics during the 8-h labeling or directly after labeling so we cannot account for changes during this time. However, changes in isotopic composition of soil organic carbon in response to the  $^{13}\text{C}$  labeling could not be observed over time or between the treatments (data not shown).

#### Effects of drought and/or heat on soil microbial groups and linkage to the plant–soil carbon continuum

In general, label was incorporated into microbial and fungal PLFAs indicated by  $^{13}\text{C}$  excess values greater

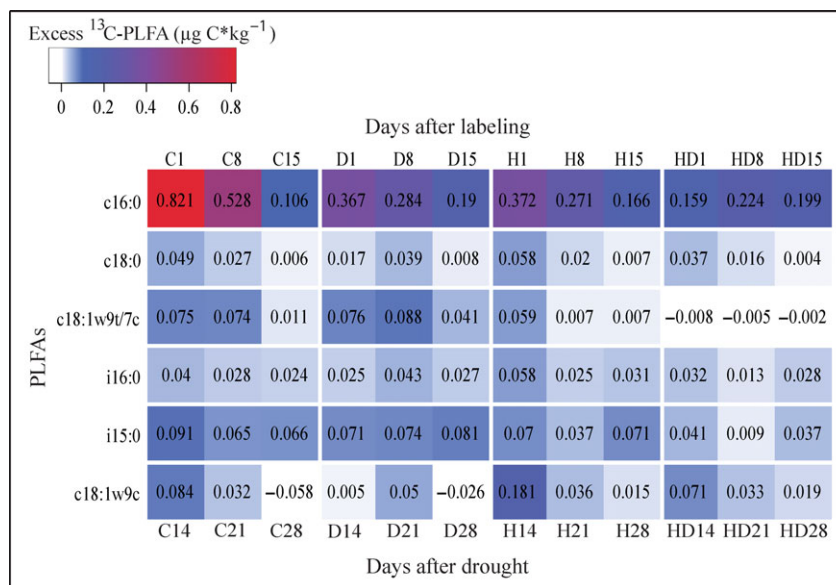


**Fig. 3** Transfer of  $^{13}\text{C}$  label to PLFAs. The heatmap shows the excess  $^{13}\text{C}$ -PLFA values ( $\mu\text{g C} \times \text{kg}^{-1}$ ) during the experiment for control (C) and treatments (D, H, HD) for different PLFAs. The upper x-axis displays days after labeling and the lower x-axis days after the onset of the drought treatment. Values are means ( $n = 5$ ).

than 0 (Fig. 3). For microbial PLFAs, the HD treatment had the largest negative impact indicated by the least  $^{13}\text{C}$  excess values. Fungal PLFAs (c18 : 1w9c) performed well in H, incorporating more label, when compared to the C and D treatment.

We analyzed 16 PLFAs to evaluate different groups of microorganisms (see Table S2 for a list of used PLFAs). The remaining PLFAs that had been extracted did not yield sufficient material for analysis (i.e., they were below the detection limit).

We chose PLFAs from each marker group except *Actinomycetes* and expressed the calculated excess  $^{13}\text{C}$ -PLFA values in a heatmap (Fig. 3). High  $^{13}\text{C}$  excess values for general PLFA markers were found in c16 : 0, c18 : 0 and c18 : 1w9t/7c with c16 : 0 having the highest values with a maximum of  $0.821 \pm \text{SE } 0.189 \mu\text{g C} \times \text{kg}^{-1}$  1 day after labeling (DD 14) in the control. There was a significant difference between one and 15 days after labeling (DD 14 and 28) for the general bacterial biomarker c16 : 0 ( $P < 0.01$ ) when considering all the treatments (Fig. 3). H and HD (but not D) were significantly different to C ( $P < 0.05$  and 0.001, respectively).

There were no significant differences in time and/or treatment for the PLFA marker of gram-positive bacteria (i16 : 0), but the excess values were positive, indicating that  $^{13}\text{C}$  was incorporated. The PLFA marker i15 : 0 (which represents heterotrophic bacteria) had the same significant differences between treatments as c18 : 1w9t/7c with HD being significantly different to C and D ( $P < 0.05$ ). The fungal PLFA c18 : 1w9c

showed higher values in H which was significantly different from C as well as D ( $P < 0.05$ ), and this marker showed a significant decrease over time when considering all treatments.

#### *Effects of drought and/or heat on the bacterial community structure*

We used the MiSeq-based sequencing of the V1–V3 region of the 16S rRNA gene to analyze the metabolically active (RNA-based) bacterial communities from five replicates per treatment. In total, 8 209 608 high-quality full-length reads were obtained. All groups of sequences were subsampled to 42 368 reads each, which was the size of the smallest sample. The total number of OTUs was 23 709 per sample, and the number of OTUs ranged from 2748 to 4642. Based on the 42 368 16S rRNA sequences per sample, a reasonable coverage of 96.6%, the mean for all samples, was achieved.

The inverse Simpson (1/D) diversity index was used to evaluate changes in bacterial diversity (Table 1) within treatments. The diversity did not change significantly within C, and we also observed only negligible changes in H and D. Similarly, species richness (number of OTUs) remained unchanged within control and treatments (Table 1). However, diversity in HD significantly decreased over time ( $P < 0.05$ ).

An NMS-based ordination for the identified OTUs was used to visualize the variability in the bacterial community and the differences in community structure

**Table 1** Richness and diversity (mean  $\pm$  SE) of OTUs based on 16S rRNA sequences for treatments at DD 0, 14 and 28 ( $n = 5$ ). The diversity index is the inverse Simpson (1/D)

Treatment	Control (C)			Drought (D)			Heat (H)			Heat-drought (HD)		
	0	14	28	0	14	28	0	14	28	0	14	28
OTU richness	4038 $\pm$ 142 <sup>a</sup>	4097 $\pm$ 167 <sup>a</sup>	4065 $\pm$ 166 <sup>a</sup>	3702 $\pm$ 198 <sup>a,b</sup>	3759 $\pm$ 149 <sup>a,b</sup>	3921 $\pm$ 254 <sup>b</sup>	3635 $\pm$ 57 <sup>c</sup>	3328 $\pm$ 170 <sup>c</sup>	3243 $\pm$ 130 <sup>c</sup>	3479 $\pm$ 95 <sup>b,c</sup>	3432 $\pm$ 142 <sup>b,c</sup>	3756 $\pm$ 157 <sup>b,c</sup>
InvSimpson	165.3 $\pm$ 13.2 <sup>a</sup>	140.4 $\pm$ 8.8 <sup>a</sup>	145.5 $\pm$ 4.7 <sup>a</sup>	130.3 $\pm$ 7.2 <sup>a,b</sup>	109.7 $\pm$ 5.7 <sup>a</sup>	137.0 $\pm$ 17.0 <sup>a,c</sup>	103.3 $\pm$ 4.2 <sup>b</sup>	131.3 $\pm$ 18.0 <sup>b</sup>	92.2 $\pm$ 4.7 <sup>b,c</sup>	104.8 $\pm$ 7.4 <sup>b</sup>	56.6 $\pm$ 6.4 <sup>b,*</sup>	56.1 $\pm$ 4.3 <sup>b,*</sup>

<sup>a,b,c</sup>Indicate significant differences between treatments.

\*Indicates significant differences between sample collection.

between the treatments (Fig. 4). D and C as well as H and HD had a similar community structure at DD 0. The community composition changed over time in C, most likely due to sampling during the tail end of the acclimation period exemplified by the relative low  $A$ -value (Table 2). The bacterial community composition in H remained unchanged, but we found a distinct shift between DD 0 vs. DD 14 and DD 28 for D and HD, with a strong initial community shift for the latter treatment. MRPP analysis further supports a clustering that distinguishes between the well-watered and drought treatments (Table 2). Thus, we found a similar trend of the community shifting between D and HD even though HD obviously had a stronger effect on the community. Remarkably, apart from the two shifts in the D and HD treatment, the bacterial community structure displayed a high tolerance.

Variability within the C and H treatment was largely due to the different monoliths. The community structure of a single monolith often clustered closely together over time; this was especially prominent for the H treatment. Thus, the community structure of monoliths 11–15 was comparable over the whole period. Even in the HD treatment where a strong shift occurred between DD 0 and DD 14, the community structure was again similar for the single monoliths 16–20 at day DD 14 and DD 28 (Fig. 4).

The analysis of phylotypes showed a high phylogenetic diversity with a total of 22 phyla. Dominant phyla were *Proteobacteria* (46%), *Actinobacteria* (18.4%), *Planctomycetes* (12.4%) and *Acidobacteria* (10.8%). We observed an increase in *Proteobacteria* in the D and HD treatment, while *Planctomycetes* decreased. *Actinobacteria* decreased only in HD. The phylotypes were analyzed to reveal taxonomic groups, which intensively responded to the treatments. In total, 31 phylotypes with a relative abundance of more than 0.1% of the bacterial community could be detected that were increased or decreased by more than 50% over time (Fig. 5). The phylotypes could be grouped based on their response to the treatments (decrease and increase in relative abundance which can be seen in the hierarchical clustering) in correspondence to their taxonomic assignment. As already seen in Fig. 5, we could detect a clear trend between bacterial phyla. Phylotypes belonging to the  $\alpha$ -,  $\beta$ - and  $\gamma$ -*Proteobacteria*, *Verrucomicrobia* and *Firmicutes* increased in relative abundance in the D and HD treatment. *Actino*- and *Acidobacteria* groups decreased only under HD and *Planctomycetes* decreased in both, D and HD. The response of these phylotypes to D and HD was consistent; thus, this response-characteristic seems to be phylogenetically highly conserved.

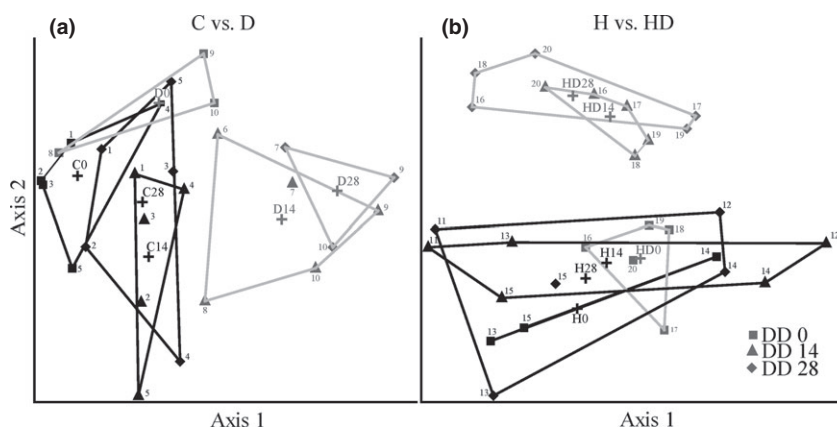


**Fig. 4** Effects of drought, a heat-pulse and heat-pulse with drought on the soil bacterial community structure. NMS ordination plots of the bacterial community structure at three different time points (DD 0, 14 and 28) for (a) control (C, black lines) vs. drought (D, gray lines) and (b) heat (H, black lines) vs. heat–drought (HD, gray lines). Numbers at points indicate different monoliths from which samples were taken; centroids are indicated by +.

**Table 2** Significance test (MRPP) of the effect of drought, a heat-pulse and a heat-pulse with drought on the bacterial community structure. *A*- and *P*-values for control (C) and treatments (D, H, HD) from the comparison of different time points (DD 0, 14 and 28) are given. Bold numbers indicate a significant *A*-value

	<i>A</i>	<i>P</i> -value
C0 : C14	<b>0.13</b>	0.021
C0 : C28	0.05	0.181
C14 : C28	−0.04	0.667
D0 : D14	<b>0.26</b>	0.007
D0 : D28	<b>0.32</b>	0.029
D14 : D28	0.01	0.391
H0 : H14	−0.06	0.671
H0 : H28	−0.06	0.626
H14 : H28	−0.08	0.988
HD0 : HD14	<b>0.34</b>	0.002
HD0 : HD28	<b>0.32</b>	0.004
HD14 : HD28	0.06	0.148

## Discussion

We designed our experiment to capture the plant–soil carbon continuum and soil microbial community responses to drought and temperature extremes. We imposed a month-long drought in which no water was supplied, and a heat-pulse (at DD 13) that lasted 8 h with maximum air temperatures of approximately 50 °C. The soil moisture stress we induced exceeded even the strong drought conditions for this part of Germany (Gimbel *et al.*, 2015). Soil water potential decreased far below the permanent wilting point, a plant physiological threshold, and below the point at which carbon substrate diffusion halts in soils, a micro-

bial environmental limitation (Manzoni *et al.*, 2011). The heat-pulse temperature was short though extreme, inducing wilting and foliar damage (Fig. S1) and may approach the temperature range of recent heat waves in Europe (Berard *et al.*, 2011).

Importantly, both the plant–soil carbon continuum and the microbial communities from soil monoliths exposed to drought (D) and a heat-pulse with drought (HD) changed significantly, thus meeting the requirement of Smith (2011) that an extreme climate event should result in a shift in ecosystem biological characteristic. Overall, we found that our treatments did not completely sever the linkages between plants and soil; however, contrasting  $\delta^{13}\text{C}$  patterns between above- and belowground tissues as well as the  $^{13}\text{C}$  in PLFAs suggest strong alterations in the linkage between photosynthesis and belowground processes among the treatments. The microbial community dynamics analyzed by PLFAs and high-throughput sequencing of the 16S rRNA were most strongly affected by the combination of a heat-pulse and drought (HD).

### Plant–soil carbon continuum

We  $^{13}\text{C}$  labeled new plant assimilates and tracked the label through the plant–soil–microorganism continuum as a proxy for the strength in coupling between aboveground plant tissues and belowground communities. As the source of labeled carbon, leaf uptake reflects the initial impact of the treatments on plants and their potential to deliver recent assimilates belowground. All treatments showed a strong  $^{13}\text{C}$  increase in leaves 1 day after labeling (DD 14), indicating that photosynthesis was still functional despite the water and heat

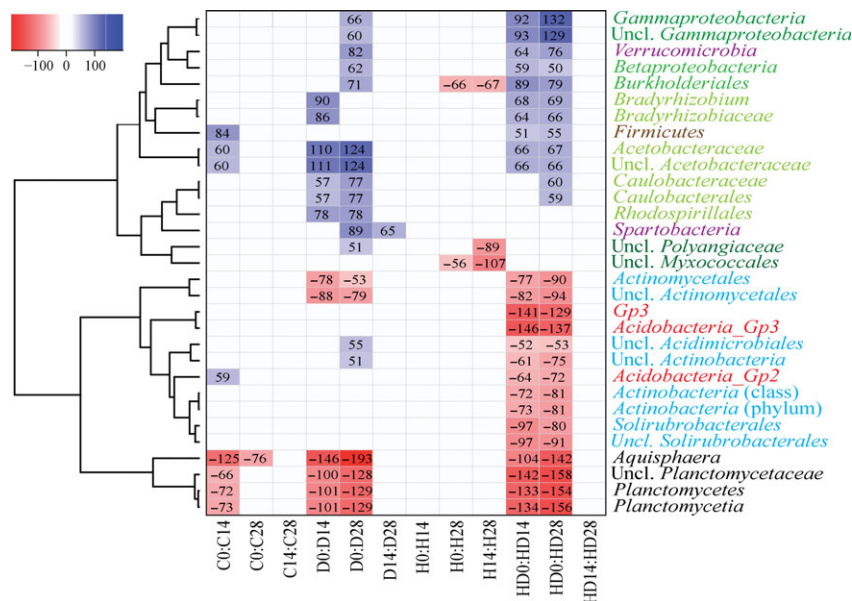


**Fig. 5** Phylotypes with abundance shifts in control (C) and treatments (H, D, HD) between three different time points (DD 0, 14, 28). Shown groups had a relative abundance of more than 0.1% of the bacterial community and increased or decreased by more than 50% over time. Values are given in % increase (blue) or decrease (red) as means. Light green to dark green = *Alpha-* to *Deltaproteobacteria*, violet = *Verrucomicrobia*, brown = *Firmicutes*, blue = *Actinobacteria*, red = *Acidobacteria*, black = *Planctomycetes*.

stress. This stress was exemplified by the significant differences between the C and D treatments. Plants experiencing drought can place a priority on maintaining hydraulic functioning (Hartmann *et al.*, 2013; Sevanto *et al.*, 2014), for example, by closing their stomata, which then leads to reduced carbon assimilation. A consequence of drought can also be decreased phloem loading and lower phloem transport velocity (Ruehr *et al.*, 2009).

The corresponding belowground patterns were different than those aboveground. The pulse of labeled carbon was present in soil CO<sub>2</sub> after 1 day in C and after 2 days in HD (Fig. S2). Based on the pattern in the HD treatment, we can infer that plants were under water stress resulting in a delay of delivery of new assimilates used for root and rhizosphere respiration (Ruehr *et al.*, 2009; Burri *et al.*, 2014). However, in all treatments, root tissue tended to increase in <sup>13</sup>C over time, indicating that labeled carbon had been allocated belowground.

The carbon continuum remained intact, although weakened, and microbial communities took up labeled carbon as well, but differences in PLFA label amount between treatments attest to their effects on the linkage between plants and soil microbial communities, thus confirming hypothesis 2. Based on the response in the control monoliths alone, there is clear indication that the potential for carbon delivery to soil microbes is high, despite sampling at a spatial scale larger than the

rhizosphere. When we consider the excess patterns of the general PLFA marker c16 : 0, which was the most enriched across all treatments, we can see that within the drought treatments the HD monoliths were more severely negatively affected.

Thus, to address Hypothesis 1, based on the arrival of label in all plant tissues and representative PLFAs, we can assert that none of the treatments were too severe to totally disrupt within-plant transport over the experiment (despite wilting in D and HD), and the depletion of the aboveground signal along with the concurrent enrichment of the belowground root tissue suggests that carbon sinks belowground were still active (Koerner, 2011; Hasibeder *et al.*, 2015). However, the stress treatments severely impaired the carbon continuum, which is readily apparent when comparing the root label patterns of the control to the stress treatments. Ultimately, the amount of label may not signify the ecological relevance of the severely impacted C continuum we observed; the relevance, rather, lies in the degree to which the microbial community was affected.

By linking the root and the PLFA label dynamics, we can detect a possible change in assimilate allocation patterns. The PLFA <sup>13</sup>C excess was generally higher in the control than in the treatments based on absolute values [e.g., c16 : 0 1 day after labeling (DD 14)], but the picture changes when the PLFA label is compared to the <sup>13</sup>C enrichment in roots (Table 3). The <sup>13</sup>C label in roots was 6.2 times higher in C compared to D 1 day

**Table 3** Relative level of  $^{13}\text{C}$  incorporation between carbon pools (roots and the general PLFA marker c16 : 0) 1 day after labeling between experimental treatments. A more equitable ratio between the compared treatments indicates the 'potential' of available carbon reaching belowground pools; in all cases, the PLFA received the largest portion of labeled carbon

C-pool	C : D	C : H	C : HD
Roots	6.2	9.8	14.8
c16 : 0 PLFA	2.2	2.2	5.1

after labeling, in comparison, the c16:0 PLFA of C exceeded D by only a factor of approx. 2.2. Similar relations were found for the H and HD treatments (Table 3). This clearly indicates that a relatively higher proportion of new assimilates arriving in roots was transferred to soil microorganisms in the water- and heat-stressed treatments.

Based on these PLFA and root patterns, we infer two pathways of carbon flow to belowground microbial communities. The first pathway is evidenced from the strong increase of label in the plant organs and  $^{13}\text{C}$  excess of PLFAs directly after labeling during non-stressed conditions, while the second pathway is apparent during environmental stress, in which the microbial pool received a higher relative proportion of labeled carbon. This may be indicative of different sink strengths or sink priorities of the carbon pool that different microbial communities (e.g., mycorrhizae) are associated with. A similar finding was observed by Hasibeder *et al.* (2015), who found that under control conditions, recent assimilates were directed to root respiration, while root respiration from plants under stress was fueled by stored carbon, possibly allocating recent assimilates to alternative belowground sinks. While assimilates may be used for root respiration under well-watered conditions or osmotic adjustment during the onset of water-stressed conditions, our results suggest that the microbial belowground community may exert a stronger sink strength during drought in which soil moisture levels exceed the plant wilting point.

#### Microbial community structure

Overall, we found the dominant taxonomic groups in our treatments were similar to other studies on forest soil (Dimitriu & Grayston, 2010; Sun *et al.*, 2014; Felsmann *et al.*, 2015), consisting of *Proteobacteria*, *Actinobacteria*, *Planctomycetes* and *Acidobacteria*. However, based on our high-throughput sequencing of the 16S rRNA, we observed multiple trajectories in the community shifts due to the stress treatments. *Planctomycetes* had the strongest negative response in our experiment (strong changes in abundance resulting in decreases

under D and HD). The phylum *Proteobacteria* performed best under the treatments with increases in relative abundance in D and HD, possibly due to a generally high soil organic carbon availability (Fierer *et al.*, 2007; Sun *et al.*, 2014) in our forest soil. The H treatment alone had no detectable effect, D had a relatively small effect, but the HD treatment had the strongest effect on the bacterial community structure with a decrease in bacterial diversity. Furthermore, most of the changes in the bacterial community occurred within the first 2 weeks of treatment, indicating that an environmental threshold might have been reached for the bacterial community.

Our findings suggest that microbial communities can tolerate a heat-pulse alone. We did not observe a significant shift in the OTU richness, diversity and community structure or changes in relative abundance of the phylotypes in Castro *et al.* (2010) found that warming does not always lead to predictable or significant changes in bacterial and fungal abundance or community structure, while Schindlbacher *et al.* (2011) suggest that heat affects major groups of soil microbial communities only when other limitations are present (e.g., water or nutrient limitation). Over a long time period of selection and evolution, microorganisms have adapted to tolerate and survive stress through a variety of different strategies (Schimel *et al.*, 2007; Wallenstein & Hall, 2012; Barnard *et al.*, 2013; Griffiths & Philippot, 2013). Thus, our heat-pulse was not strong enough to see an immediate effect. This is congruent to the high tolerance that we found for the microbial community in our soils; however, even though we did not observe a change in the bacterial community structure in the H treatment, a delayed stress response is still possible (e.g., through large shifts in the allocation of C and N) (Schimel *et al.*, 2007).

The bacterial communities were more or less tolerant to the D treatment, contradicting our original expectation, and we found only minor changes in the community structure relative to the control. Furthermore, we were not able to detect significant differences in richness and diversity of the bacterial communities within this treatment. Over the course of the experiment, we found that the relative abundance of the phylum *Proteobacteria* increased and *Planctomycetes* decreased, but we observed a similar though lower trend in C. We infer from these patterns that species that performed poorly under drought (e.g., bacteria from the phylum of *Planctomycetes*) were out-competed by more tolerant species (e.g., from the phylum of *Proteobacteria*), and thus, a diversity or species richness change was not observed within the shifting community. There was also a slight yet significant increase in the *Actinobacteria* relative abundance in D. Numerous members of

*Actinobacteria* are known to compete well under dry conditions (Barnard *et al.*, 2013; Felsmann *et al.*, 2015). Filamentous (mycelium-forming) *Actinobacteria* use this growth form to facilitate growth and expansion under conditions of low hydraulic connectivity (drought conditions) in unsaturated soils (Wolf *et al.*, 2013), which could be an explanation for stimulated growth under moderate drought conditions.

The mixed response of bacterial communities to drought in our experiment clearly reflects the different physiological strategies (often accompanied by a change in community composition) microorganisms have developed to cope with drought stress. Physiological strategies for drought include production of protective molecules, dormancy or higher carbon use efficiency (Schimel *et al.*, 2007). Soil microorganisms also have on average a relatively dry optimum (−320 kPa) and are capable of respiring even under lower water potentials (−2000 MPa) displaying a broad range of moisture tolerance (Lennon *et al.*, 2012). However, our study imposed extreme environmental conditions carried out over several weeks and thus only gives a short-term perspective of microbial community shifts. Over the long term, microbial community shifts may also be driven by ecosystem feedbacks to drought, such as changes in soil C/N ratio, pH and nitrogen input (Evans *et al.*, 2013).

The strongest change in the active microbial community was in the HD treatment, which had a clear negative effect on diversity (only in HD did we see a significant decrease in diversity) and resulted in a distinct shift in the community structure and changes in relative abundance of many phylotypes. In the HD treatment, *Planctomycetes*, *Actinobacteria* and *Acidobacteria* were the phylotypes most affected and had the largest decrease in relative abundances. Interestingly, many of the starkest changes in abundances occurred in HD in which the plant community suffered the most; furthermore, these changes did not occur in C, D or H. We infer from this finding that the indirect effects of the treatment on the microbial pattern resulted in the largest community shift, confirming hypothesis 3; however, our experimental design excludes the possibility to test solely for direct effects of the treatment on the microbial communities. This pattern also corresponds clearly to the low level of label in the <sup>13</sup>C PLFAs we found in HD compared to the other treatments. Thus, our data suggest that *Actinobacteria* and members of *Acidobacteria* are more tightly linked to the fate of plants and their carbon delivery during environmental stress (i.e., the indirect climate change effect). Furthermore, the corresponding increase in relative abundance of the *Alpha*- and *Gammaproteobacteria* suggests that members within these phyla were able to take advantage of the

altered belowground conditions that occurred with the plant stress response (e.g., reduced carbon transfer belowground).

Our results reinforce current observations of a diverse microbial response to environmental stress in which members of various phyla exhibit optima during moderate-to-dry moisture conditions (Lennon *et al.*, 2012; Barnard *et al.*, 2013). Given that a subset of phyla responded similarly (i.e., in trajectory but not magnitude) in D and HD, we can conclude that the resistance mechanisms under the direct climate change effects of drought and increased temperature are phylogenetically highly conserved. In the same breath, our understanding of the microbial response to environmental stress has also expanded. Our study exemplifies that many of the shifts in the microbial communities that we might expect from climate change will result from the plant–soil–microbial dynamics rather than from direct effects on soil microbes alone. In particular, the plant's role in carbon delivery belowground is critical for some phyla, and as our data suggest, these microbes may maintain belowground pools as a carbon sink priority even for stressed plants. The plant–soil–microorganism relationship is fundamental to terrestrial ecosystems globally, and advances in understanding or predicting balances of energy and nutrient fluxes or alterations of microbial diversity under global climate change will clearly depend on our ability to accurately characterize this relationship.

### Acknowledgements

Special thanks go to all those who helped excavate the monoliths: Kai Nitzsche, Katharina Sliwinski, Qirui Li, Marcus Fahle, Martin Schmidt, Leonardt Mayer and Anna Rosner. We are grateful to Herbert Lauberbach from the forest district Kammerforst for permission to extract monoliths from the site. We thank Sigune Weinert for her technical assistance in molecular analyses, Frau Remus for her help in isotope analyses and Norbert Wypler for pF curve measurements. We also acknowledge Stacie Kageyama for discussions concerning the analyses and three anonymous reviewers for very helpful and insightful comments on a previous version of this manuscript.

### References

- Aerts R (1997) Climate, leaf litter chemistry and leaf litter decomposition in terrestrial ecosystems: a triangular relationship. *Oikos*, **79**, 439–449.
- Allison SD, Wallenstein MD, Bradford MA (2010) Soil-carbon response to warming dependent on microbial physiology. *Nature Geoscience*, **3**, 336–340.
- Bahn M, Reichstein M, Dukes JS, Smith MD, McDowell NG (2014) Climate–biosphere interactions in a more extreme world. *New Phytologist*, **202**, 356–359.
- Barcnas-Moreno G, Gomez-Brandon M, Rousk J, Baath E (2009) Adaptation of soil microbial communities to temperature: comparison of fungi and bacteria in a laboratory experiment. *Global Change Biology*, **15**, 2950–2957.
- Bardgett RD, Bowman WD, Kaufmann R, Schmidt SK (2005) A temporal approach to linking aboveground and belowground ecology. *Trends in Ecology & Evolution*, **20**, 634–641.

- Bardgett RD, Freeman C, Ostle NJ (2008) Microbial contributions to climate change through carbon cycle feedbacks. *The ISME Journal*, **2**, 805–814.
- Barnard RL, Osborne CA, Firestone MK (2013) Responses of soil bacterial and fungal communities to extreme desiccation and rewetting. *The ISME Journal*, **7**, 2229–2241.
- Beniston M, Stephenson DB, Christensen OB *et al.* (2007) Future extreme events in European climate: an exploration of regional climate model projections. *Climatic Change*, **81**, 71–95.
- Berard A, Bouchet T, Sévenier G, Pablo A-L, Gros R (2011) Resilience of soil microbial communities impacted by severe drought and high temperature in the context of Mediterranean heat waves. *European Journal of Soil Biology*, **47**, 333–342.
- Bonkowski M, Roy J (2005) Soil microbial diversity and soil functioning affect competition among grasses in experimental microcosms. *Oecologia*, **143**, 232–240.
- Boschker HTS, Kromkamp JC, Middelburg JJ (2005) Biomarker and carbon isotopic constraints on bacterial and algal community structure and functioning in a turbid, tidal estuary. *Limnology and Oceanography*, **50**, 70–80.
- Briffa K, van der Schrier G, Jones P (2009) Wet and dry summers in Europe since 1750: evidence of increasing drought. *International Journal of Climatology*, **29**, 1894–1905.
- Burri S, Sturm P, Prechsl UE, Knohl A, Buchmann N (2014) The impact of extreme summer drought on the short-term carbon coupling of photosynthesis to soil CO<sub>2</sub> efflux in a temperate grassland. *Biogeosciences*, **11**, 961–975.
- Castro HF, Classen AT, Austin EE, Norby RJ, Schadt CW (2010) Soil microbial community responses to multiple experimental climate change drivers. *Applied and Environmental Microbiology*, **76**, 999–1007.
- Ciais P, Reichstein M, Viovy N *et al.* (2005) Europe-wide reduction in primary productivity caused by the heat and drought in 2003. *Nature*, **437**, 529–533.
- Clark JM, Chapman PJ, Adamson JK, Lane SN (2005) Influence of drought-induced acidification on the mobility of dissolved organic carbon in peat soils. *Global Change Biology*, **11**, 791–809.
- Clarke KR (1993) Non-parametric multivariate analyses of changes in community structure. *Australian Journal of Ecology*, **18**, 117–143.
- Crowther TW, Maynard DS, Leff JW, Oldfield EE, McCulley RL, Fierer N, Bradford MA (2014) Predicting the responsiveness of soil biodiversity to deforestation: a cross-biome study. *Global Change Biology*, **20**, 2983–2994.
- Csonka LN (1989) Physiological and genetic responses of bacteria to osmotic stress. *Microbiological Reviews*, **53**, 121–147.
- Denef K, Roobroeck D, Manimel Wadu MCW, Lootens P, Boeckx P (2009) Microbial community composition and rhizodeposit-carbon assimilation in differently managed temperate grassland soils. *Soil Biology and Biochemistry*, **41**, 144–153.
- Dimitriu PA, Grayston SJ (2010) Relationship between soil properties and patterns of bacterial beta-diversity across reclaimed and natural boreal forest soils. *Microbial Ecology*, **59**, 563–573.
- Edgar RC (2013) UPARSE: highly accurate OTU sequences from microbial amplicon reads. *Nature Methods*, **10**, 996–998.
- Edgar RC, Haas BJ, Clemente JC, Quince C, Knight R (2011) UCHIME improves sensitivity and speed of chimera detection. *Bioinformatics*, **27**, 2194–2200.
- Evans SE, Wallenstein MD (2014) Climate change alters ecological strategies of soil bacteria. *Ecology Letters*, **17**, 155–164.
- Evans SE, Wallenstein MD, Burke IC (2013) Is bacterial moisture niche a good predictor of shifts in community composition under long-term drought? *Ecology*, **95**, 110–122.
- Felsmann K, Baudis M, Gimbel K *et al.* (2015) Soil bacterial community structure responses to precipitation reduction and forest management in forest ecosystems across Germany. *PLoS One*, **10**, e0122539.
- Fierer N, Bradford MA, Jackson RB (2007) Toward an ecological classification of soil bacteria. *Ecology*, **88**, 1354–1364.
- Fischer EM, Schar C (2010) Consistent geographical patterns of changes in high-impact European heatwaves. *Nature Geoscience*, **3**, 398–403.
- Fischer M, Bossdorf O, Gockel S *et al.* (2010) Implementing large-scale and long-term functional biodiversity research: the Biodiversity Exploratories. *Basic and Applied Ecology*, **11**, 473–485.
- Flexas J, Bota J, Galmés J, Medrano H, Ribas-Carbo M (2006) Keeping a positive carbon balance under adverse conditions: responses of photosynthesis and respiration to water stress. *Physiologia Plantarum*, **127**, 343–352.
- Frey SD, Drijber R, Smith H, Melillo J (2008) Microbial biomass, functional capacity, and community structure after 12 years of soil warming. *Soil Biology and Biochemistry*, **40**, 2904–2907.
- Frostegård Å, Tunlid A, Bååth E (1991) Microbial biomass measured as total lipid phosphate in soils of different organic content. *Journal of Microbiological Methods*, **14**, 151–163.
- Fuchslueger L, Bahn M, Fritz K, Hasibeder R, Richter A (2014) Experimental drought reduces the transfer of recently fixed plant carbon to soil microbes and alters the bacterial community composition in a mountain meadow. *The New Phytologist*, **201**, 916–927.
- Gilliam FS, Hédli R, Chudomelová M, McCulley RL, Nelson JA (2014) Variation in vegetation and microbial linkages with slope aspect in a montane temperate hardwood forest. *Ecosphere*, **5**, art66–art66.
- Gimbel KF, Felsmann K, Baudis M *et al.* (2015) Drought in forest understory ecosystems – a novel rainfall reduction experiment. *Biogeosciences*, **12**, 961–975.
- Griffiths BS, Philippot L (2013) Insights into the resistance and resilience of the soil microbial community. *FEMS Microbiology Reviews*, **37**, 112–129.
- Hartmann H, Ziegler W, Kolle O, Trumbore S (2013) Thirst beats hunger—declining hydration during drought prevents carbon starvation in Norway spruce saplings. *New Phytologist*, **200**, 340–349.
- Hasibeder R, Fuchslueger L, Richter A, Bahn M (2015) Summer drought alters carbon allocation to roots and root respiration in mountain grassland. *New Phytologist*, **205**, 1117–1127.
- Hobbie SE (1992) Effects of plant species on nutrient cycling. *Trends in Ecology & Evolution*, **7**, 336–339.
- Hommel R, Siegwolf R, Saurer M, Farquhar GD, Kayler Z, Ferrio JP, Gessler A (2014) Drought response of mesophyll conductance in forest understory species – impacts on water-use efficiency and interactions with leaf water movement. *Physiologia Plantarum*, **152**, 98–114.
- Hoover D, Knapp A, Smith M (2014) Resistance and resilience of a grassland ecosystem to climate extremes. *Ecology*, **95**, 2646–2656.
- Huse SM, Welch DM, Morrison HG, Sogin ML (2010) Ironing out the wrinkles in the rare biosphere through improved OTU clustering. *Environmental Microbiology*, **12**, 1889–1898.
- IPCC (2012) *Managing the Risks of Extreme Events and Disasters to Advance Climate Change Adaptation. A Special Report of Working Groups I and II of the Intergovernmental Panel of Climate Change* (eds Field CB, Barros V, Stocker TF, Qin D, Dokken DJ, Ebi KL, Mastrandrea MD, Mach KJ, Plattner G-K, Allen SK, Tignor M, Midgley PM). Cambridge University Press, Cambridge, UK and New York, USA.
- Kaur A, Chaudhary A, Kaur A, Choudhary R, Kaushik R (2005) Phospholipid fatty acid – a bioindicator of environment monitoring and assessment in soil ecosystem. *Current Science*, **89**, 1103–1112.
- Kayler ZE, De Boeck HJ, Fatchi S *et al.* (2015) Experiments to confront the environmental extremes of climate change. *Frontiers in Ecology and the Environment*, **13**, 219–225.
- Koerner C (2011) The grand challenges in functional plant ecology. *Frontiers in Plant Science*, **2**, 1–3.
- Lau JA, Lennon JT (2011) Evolutionary ecology of plant–microbe interactions: soil microbial structure alters selection on plant traits. *New Phytologist*, **192**, 215–224.
- Lennon JT, Aanderud ZT, Lehmkuhl BK, Schoolmaster DR (2012) Mapping the niche space of soil microorganisms using taxonomy and traits. *Ecology*, **93**, 1867–1879.
- Litton CM, Raich JW, Ryan MG (2007) Carbon allocation in forest ecosystems. *Global Change Biology*, **13**, 2089–2109.
- Manzoni S, Schimel JP, Porporato A (2011) Responses of soil microbial communities to water stress: results from a meta-analysis. *Ecology*, **93**, 930–938.
- Manzoni S, Schaeffer SM, Katul G, Porporato A, Schimel JP (2014) A theoretical analysis of microbial eco-physiological and diffusion limitations to carbon cycling in drying soils. *Soil Biology and Biochemistry*, **73**, 69–83.
- McCune B, Mefford MJ (2011) *PC-ORD: Multivariate Analysis of Ecological Data Version 4*. MjM Software Design, Gleneden Beach, Oregon.
- McCune B, Grace JB, Urban DL (2002) *Analysis of ecological communities*. MjM Software Design, Gleneden Beach, Oregon. 304 p.
- Menzel A, Sparks TIMH, Estrella N *et al.* (2006) European phenological response to climate change matches the warming pattern. *Global Change Biology*, **12**, 1969–1976.
- Merilä J, Hendry AP (2014) Climate change, adaptation, and phenotypic plasticity: the problem and the evidence. *Evolutionary Applications*, **7**, 1–14.
- Mielke PW, Berry KJ (2007) *Permutation Methods: A Distance Function Approach*. Springer Science & Business Media, Springer-Verlag, New York.
- Placella SA, Brodie EL, Firestone MK (2012) Rainfall-induced carbon dioxide pulses result from sequential resuscitation of phylogenetically clustered microbial groups. *Proceedings of the National Academy of Sciences*, **109**, 10931–10936.
- Prescott CE, Grayston SJ (2013) Tree species influence on microbial communities in litter and soil: current knowledge and research needs. *Forest Ecology and Management*, **309**, 19–27.
- R Development Core Team (2008) *R: A Language and Environment for Statistical Computing*. R Foundation for Statistical Computing, Vienna, Austria.
- Reichstein M, Bahn M, Ciais P *et al.* (2013) Climate extremes and the carbon cycle. *Nature*, **500**, 287–295.

- Resco V, Ewers BE, Sun W, Huxman TE, Weltzin JF, Williams DG (2009) Drought-induced hydraulic limitations constrain leaf gas exchange recovery after precipitation pulses in the C3 woody legume, *Prosopis velutina*. *New Phytologist*, **181**, 672–682.
- Riah-Anglet W, Trinsoutrot-Gattin I, Martin-Laurent F, Laroche-Ajzenberg E, Norini M-P, Latour X, Laval K (2015) Soil microbial community structure and function relationships: a heat stress experiment. *Applied Soil Ecology*, **86**, 121–130.
- Ruehr NK, Offermann CA, Gessler A, Winkler JB, Ferrio JP, Buchmann N, Barnard RL (2009) Drought effects on allocation of recent carbon: from beech leaves to soil CO<sub>2</sub> efflux. *The New Phytologist*, **184**, 950–961.
- Schar C, Vidale PL, Luthi D, Frei C, Haberli C, Liniger MA, Appenzeller C (2004) The role of increasing temperature variability in European summer heatwaves. *Nature*, **427**, 332–336.
- Scheffer M, Carpenter SR (2003) Catastrophic regime shifts in ecosystems: linking theory to observation. *Trends in Ecology & Evolution*, **18**, 648–656.
- Schimel J, Schaeffer SM (2012) Microbial control over carbon cycling in soil. *Frontiers in Microbiology*, **3**, 348.
- Schimel J, Balser TC, Wallenstein M (2007) Microbial stress-response physiology and its implications for ecosystem function. *Ecology*, **88**, 1386–1394.
- Schindlbacher A, Rodler A, Kuffner M, Kitzler B, Sessitsch A, Zechmeister-Boltenstern S (2011) Experimental warming effects on the microbial community of a temperate mountain forest soil. *Soil Biology and Biochemistry*, **43**, 1417–1425.
- Schloss PD, Westcott SL, Ryabin T *et al.* (2009) Introducing mothur: open-source, platform-independent, community-supported software for describing and comparing microbial communities. *Applied and Environmental Microbiology*, **75**, 7537–7541.
- Schloss PD, Gevers D, Westcott SL (2011) Reducing the effects of PCR amplification and sequencing artifacts on 16S rRNA-based studies. *PLoS One*, **6**, e27310.
- Schnitzer SA, Klironomos J (2011) Soil microbes regulate ecosystem productivity and maintain species diversity. *Plant Signaling & Behavior*, **6**, 1240–1243.
- Schnitzer SA, Klironomos JN, HilleRisLambers J *et al.* (2010) Soil microbes drive the classic plant diversity–productivity pattern. *Ecology*, **92**, 296–303.
- Seki K (2007) SWRC fit? A nonlinear fitting program with a water retention curve for soils having unimodal and bimodal pore structure. *Hydrology and Earth System Sciences Discussions Discussions*, **4**, 407–437.
- Sevanto S, McDowell NG, Dickman LT, Pangle R, Pockman WT (2014) How do trees die? A test of the hydraulic failure and carbon starvation hypotheses. *Plant, Cell & Environment*, **37**, 153–161.
- Shade A, Peter H, Allison SD *et al.* (2012) Fundamentals of microbial community resistance and resilience. *Frontiers in Microbiology*, **3**, 417.
- Smith MD (2011) An ecological perspective on extreme climatic events: a synthetic definition and framework to guide future research. *Journal of Ecology*, **99**, 656–663.
- Steger K, Premke K, Gudaszc C, Sundh I, Tranvik LJ (2011) Microbial biomass and community composition in boreal lake sediments. *Limnology and Oceanography*, **56**, 725–733.
- Sun H, Terhonen E, Koskinen K, Paulin L, Kasanen R, Asiegbu FO (2014) Bacterial diversity and community structure along different peat soils in boreal forest. *Applied Soil Ecology*, **74**, 37–45.
- Van Der Heijden MGA, Bardgett RD, Van Straalen NM (2008) The unseen majority: soil microbes as drivers of plant diversity and productivity in terrestrial ecosystems. *Ecology Letters*, **11**, 296–310.
- Van Genuchten MT (1980) A closed-form equation for predicting the hydraulic conductivity of unsaturated soils. *Soil Science Society of America Journal*, **44**, 892–898.
- Wagg C, Bender SF, Widmer F, van der Heijden MGA (2014) Soil biodiversity and soil community composition determine ecosystem multifunctionality. *Proceedings of the National Academy of Sciences*, **111**, 5266–5270.
- Waldrop MP, Firestone MK (2006) Response of microbial community composition and function to soil climate change. *Microbial Ecology*, **52**, 716–724.
- Wallenstein MD, Hall EK (2012) A trait-based framework for predicting when and where microbial adaptation to climate change will affect ecosystem functioning. *Biogeochemistry*, **109**, 35–47.
- Walther G-R, Post E, Convey P *et al.* (2002) Ecological responses to recent climate change. *Nature*, **416**, 389–395.
- Wolf AB, Vos M, de Boer W, Kowalchuk GA (2013) Impact of matric potential and pore size distribution on growth dynamics of filamentous and non-filamentous soil bacteria. *PLoS One*, **8**, e83661.

### Supporting Information

Additional Supporting Information may be found in the online version of this article:

**Table S1.** Information on plant species found on the monoliths.

**Table S2.** Phospholipid fatty acids (PLFAs) that were used as markers for certain groups of microorganisms in the experiment.

**Figure S1.** Pictures of heat-pulse with drought (HD) monoliths.

**Figure S2.**  $\delta^{13}\text{C}_{\text{CO}_2}$  values (‰) inside the chamber during labeling (inset graph) and gas within the soil for five days after labeling.